

Systematic understanding of half-metallicity of ternary compounds in Heusler and Inverse Heusler structures with 3d and 4d elements.

Srikrishna Ghosh¹ and Subhradip Ghosh^{1,*}

¹*Department of Physics, Indian Institute of Technology Guwahati, Guwahati-781039, Assam, India.*

(Dated: February 4, 2022)

Employing *ab initio* electronic structure calculations we extensively study ternary Heusler compounds having the chemical formula $X_2X'Z$, where $X = \text{Mn, Fe or Co}$; $Z = \text{Al or Si}$; and X' changes along the row of 4d transition metals. A comprehensive overview of these compounds, addressing the trends in structural, electronic, magnetic properties and Curie temperature is presented here along with the search for new materials for spintronics applications. A simple picture of hybridization of the d orbitals of the neighboring atoms is used to explain the origin of the half-metallic gap in these compounds. We show that arrangements of the magnetic atoms in different Heusler lattices are largely responsible for the interatomic exchange interactions that are correlated with the features in their electronic structures as well as possibility of half-metallicity. We find seven half-metallic magnets with 100% spin polarization. We identify few other compounds with high spin polarisation as “near half-metals” which could be of potential use in applications as well. We find that the major features in the electronic structures remain intact if a 3d X' constituent is replaced with an isoelectronic 4d, implying that the total number of valence electrons can be used as a predictor of half-metallic nature in compounds from Heusler family.

PACS numbers:

I. INTRODUCTION

Since the discovery in 1903, Heusler alloys have been exhaustively studied for its numerous potential applications. A variety of diverse magnetic phenomena ranging from half-metallicity, magnetic shape-memory effect, giant magnetocaloric effect, thermoelectric effect, spin-light emitting diode^{1–7} to recently discovered Spin gapless semiconductor, topological insulators, superconductivity, multifunctional Heuslers for recording^{8–12} have been identified in some of the Heusler groups, comprising more than thousand compounds.

Among the explored intermetallics, full Heuslers ($L2_1$) X_2YZ are largest in number, where X and Y are transition metal and Z is a main group element. It is obvious that the unfilled d -shells of more than one transition metal elements give rise to the novel magnetic properties of these Heusler alloys. The occupancies of the transition metal magnetic elements in sub-lattices with various symmetries, the magnetic structure associated with and the resulting electronic structures are responsible for the novel properties in these materials.

Search for half-metals (HM) and spin gapless semiconductors (SGS) has been one of the forerunning research area in condensed matter physics due to these materials being suitable for spintronics applications. Extensive investigations on Heusler compounds, towards this direction, has paid rich dividends as quite a few HM and SGS have been discovered with composition X_2YZ where X and Y are elements from the 3d series of periodic table^{13–19}. The investigations into compounds with either both X and Y are elements with 4d electrons or one of them a 4d element are fewer in number. Presence of both 3d and 4d magnetic elements in the same compound with Heusler structure is expected to provide interesting perspectives. However, there is no systematic investiga-

tions available in Heusler compounds having both 3d and 4d elements.

In this paper, we, therefore, have tried to explore six ternary series $X_2X'Z$, with $X = \text{Mn, Fe, Co}$, $Z = \text{Al, Si}$ while X' is varied from Y to Ag down the series in the periodic table by Density functional theory (DFT) based electronic structure calculations. Among the family of ternary Heusler compounds Co_2 and Mn_2 -based Heusler compounds have drawn commendable interest for applications in the areas of spintronics and other magnetism related applications due to their high Curie temperatures^{18,20–22}. Fe-based Heusler compounds are known to be soft ferromagnets with Curie temperature as high as 900 K making them suitable for potential magnetic applications²³. Thus, we find it intriguing to explore specifically Mn_2 , Fe_2 and Co_2 based ternary alloys for the search of new materials with one magnetic element being one with 4d electrons, for spintronics applications. Apart from the quest for new half-metallic magnets our motivations for this work are the following:

(1) to understand the effects and their origin, of the presence of an element with 4d electrons on the structure, electronic and magnetic properties of ternary compounds where the other magnetic elements are from 3d transition metal series. A systematic study spanning across several Heusler series would help understand the comparative roles of 4d and 3d elements.

(2) to understand the effects and their origin, of replacing an element with 3d electrons by an element with 4d electrons on the electronic and magnetic properties in the context of half-metallicity.

(3) to understand the impacts and their origin, of replacing the main group element Si with Al in case of ternary alloys having both 3d and 4d elements as magnetic components.

The paper is organised as follows: Computational de-

tails and the methods, used in this work are given in the next section. In the subsequent section (Section III) we present the discussions of the calculated results on structural, electronic and magnetic properties of the ternary compounds mentioned above along with a comparative understanding with compounds having only 3d elements as the magnetic components. The conclusions and future outlook is presented at the end.

II. COMPUTATIONAL DETAILS

We have used spin-polarized DFT based projector augmented wave methods as implemented in Vienna Ab-initio Simulation Package (VASP)^{24–26} with Generalized Gradient Approximation (GGA)²⁷ for calculating electronic structure. An energy cut-off of 450 eV and a Monkhorst-Pack²⁸ 25 x 25 x 25 k-mesh was used for self-consistent calculations while a larger 31 x 31 x 31 k-mesh was used for calculating densities of states. We set the energy and the force convergence criteria to 10^{-6} eV and 10^{-2} eV/Å respectively.

With multiple scattering Green function formalism as implemented in SPRKKR code²⁹ we have calculated the magnetic pair exchange parameters. Here, the spin part of the Hamiltonian is mapped to a Heisenberg model

$$H = - \sum_{\mu, \nu} \sum_{i, j} J_{\mu\nu}^{ij} \mathbf{e}_{\mu}^i \cdot \mathbf{e}_{\nu}^j$$

where μ, ν represent different sub-lattices, i, j represent atomic positions and \mathbf{e}_{μ}^i denotes the unit vector along the direction of magnetic moments at site i belonging to sub-lattice μ . The $J_{\mu\nu}^{ij}$ are calculated from the energy differences due to infinitesimally small orientations of a pair of spins within the formulation of Liechtenstein *et. al.*³⁰. Full potential spin polarized scalar relativistic Hamiltonian with angular momentum cut-off $l_{max} = 3$ is used to calculate the energy differences by the SPRKKR code. We have used a uniform k-mesh of $22 \times 22 \times 22$ for Brillouin zone integrations. The Green's functions were calculated for 32 complex energy points distributed on a semiconductor contour. For the self-consistence cycles, the energy convergence criterion was set to 10^{-6} Ry. The calculated $J_{\mu\nu}^{ij}$ were used further to compute the Curie temperatures within the mean field approximation³¹.

III. RESULTS AND DISCUSSIONS

A. Structural Properties

$X_2X'Z$ ternary Heusler alloys crystallise in two prototype structures. The “regular” Heusler or $L2_1$ (Cu_2MnAl prototype) crystallises in a cubic structure with the space group $Fm\bar{3}m$ (space group number 225). The other one, the “inverse” Heusler, has the prototype Hg_2CuTi (space group number 216; $F\bar{4}3m$) structure. The structures are schematically shown in Fig 1.

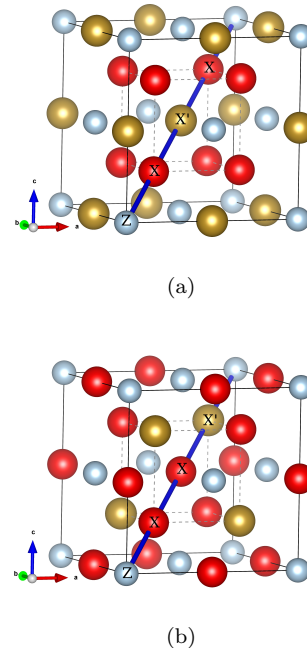


FIG. 1: Crystal structure of ternary Heusler compounds $X_2X'Z$ in (a) T_I (Heusler *i.e* two X atoms are in symmetric positions) (b) T_{II} (Inverse Heusler *i.e* X and X' are in symmetric positions).

In $L2_1$ structure the Wyckoff positions $4a(0,0,0)$ and $4b(1/2, 1/2, 1/2)$ are occupied by the least and the most electronegative elements X' and Z respectively forming a rocksalt (NaCl) type lattice. The $8c$ Wyckoff positions $(1/4, 1/4, 1/4)$ are occupied by two X atoms as shown in Fig.1.(a). Since the interaction between X' and Z atoms are ionic in character, they are octahedrally coordinated. The tetrahedral voids are filled up with X atoms, having electronegativity in between those of X' and Z . In inverse Heusler structure, X atoms of $X_2X'Z$ compounds sit at the Wyckoff positions $4b(1/2, 1/2, 1/2)$ and $4c(1/4, 1/4, 1/4)$, whereas $4a(0,0,0)$ and $4d(3/4, 3/4, 3/4)$ are occupied by Z and X' atoms respectively¹⁹ as shown in Fig.1.(b).

In Table I we present the structural properties (the crystal structure type and the lattice constant) of the lowest energy Heusler phases, obtained by our calculations, for the compounds considered here. The trends in the structure types can be understood from the following empirical rule based on the electronegativities of the constituents which has been successful in explaining the structural preferences for a number of Heusler intermetallics^{32–44}: if the main group element is fixed at $4a$ site, the $4b$ site should be occupied by the least electronegative element of the remaining three transition metal atoms⁴⁵. From our results, we find that except Mn_2NbZ , $X_2\text{Mo}'Z$ ($X = \text{Mn, Fe, Co}$) and Co_2TcAl this rule explains the structure types for all other compounds. The computed lattice constants agree well with the existing results. In case of lattice constants, we find that

the lattice constants of ternary Heuslers are greater when X' is an element with $4d$ electrons, in comparison to its counterpart with X' an element with $3d$ electrons located right above the column in periodic table (Table I, supplementary material). This trend can be explained purely on the basis of relative sizes of the atomic radii of the X' component.

In order to first verify whether a compound indeed can be formed, we have calculated the formation energies the following way:

$$E_f = E_{X_2X'Z} - (2E_X + E_{X'} + E_Z)$$

Where $E_{X_2X'Z}$ is the total energies per formula unit of the $X_2X'Z$ and E_X , $E_{X'}$, E_Z , are the total energies of the bulk X , X' and Z respectively in their ground state structures. The results are tabulated in Table I. Except Fe_2AgAl , Mn_2AgSi and Fe_2AgSi most compounds are likely to form as the formation energies are negative and hence are thermally stable from the point of view of Enthalpy. Thus, it is worth investigating further the properties of all these ternary Heusler compounds.

B. The Magnetic moments and the Slater-Pauling Rule

The necessary condition for a Heusler alloy to be half-metal is that the total spin-magnetic moment per formula-unit is an integer and that it follows the Slater-Pauling rule, connecting the magnetic moment to the total number of valence electrons per formula unit^{51–54}. In case of half-metallic ternary Heusler alloys $X_2X'Z$, the manifestation of this rule is that the total magnetic moment per formula unit, M and the number of valence electrons per formula unit, N_V are related by $M = |N_V - 18|$ or by $M = |N_V - 24|$ or by $M = |N_V - 28|$, depending on whether X is an early transition metal; or more precisely whether the Fermi-energy is placed in a gap after 9, 12 or 14 electronic states respectively^{4,53}. In Fig 2.(a), we have plotted the variations of M with N_V for $X_2X'\text{Al}$ ($X' = 4d$, $X = \text{Mn, Fe, Co}$). Our results show that the moments of $\text{Mn}_2X'Z$ compounds follow the $M = |N_V - 24|$ rule with the exceptions of Mn_2YAl , Mn_2PdZ and Mn_2AgZ where the expected moments are smaller than those predicted by the Slater-Pauling rule. However, the moment of Mn_2PdAl lies close to $M = |N_V - 28|$ line. For $\text{Fe}_2X'Z$ series we find that for compounds with X' an element after Mo , the moments of all compounds are much deviated from any of the Slater-Pauling lines. In case of $\text{Co}_2X'\text{Al}$ series the moments deviate from the line $M = |N_V - 24|$ for late transition metals ($X' = \text{Ru, Rh, Pd, Ag}$), though Co_2PdAl lies close to $M = |N_V - 28|$ line. For the case of $\text{Co}_2X'\text{Si}$ series except Co_2YSi and Co_2ZrSi none of the compounds follow the $M = |N_V - 24|$ rule. Co_2MoSi with 28 valence electrons and having total moment zero lies on $M = |N_V - 28|$. Across the six series under investigation there are only two compounds, Mn_2ZrAl and Mn_2YSi having moments in conformation

with both $M = |N_V - 18|$ and $M = |N_V - 24|$ rules. In principle these system can have gaps after both 9 states and 12 states⁵⁵.

Fig 2 and Table I demonstrate that there are quite a few compounds with integer or close to integer moments following Slater-Pauling rule. These are the potential half-metals whose electronic structures need to be examined carefully before coming to any conclusion. In the next sub-section we discuss in detail the electronic structures of compounds in each series and try to understand the origin of half-metallicity in compounds with $4d$ elements.

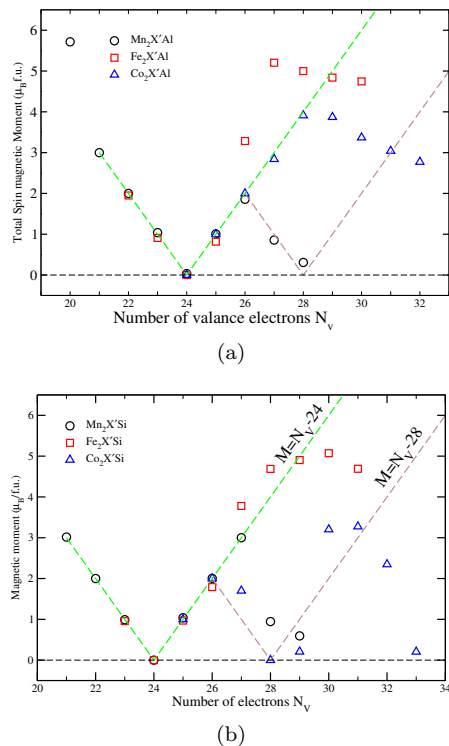


FIG. 2: Total magnetic moments versus the total number of valence electrons N_V for (a) $X_2X'\text{Al}$ and (b) $X_2X'\text{Si}$ compounds respectively. The Slater-Pauling $M = N_V - 24$ and $M = N_V - 28$ lines are drawn as a guide to understand whether the compounds follow Slater-Pauling rule.

C. Electronic Structure

The origin of the half-metallic gap and the conformation to the Slater-Pauling rule by magnetic Heusler and inverse Heusler alloys can be understood from their electronic structures near the Fermi level by addressing the hybridisations between the constituents of the compounds^{4,53,56}. In a ternary Heusler compound $X_2X'Z$, the sp -element Z provides 4 low lying (below d bands) states—one s and three p - in each spin channel. These $s-p$ bands lie well below the Fermi-energy, accommodate charges from the atoms with d electrons and stabilize the structure². The d -orbitals of transition-metal

TABLE I: Calculated lattice constants, formation energies, structure type and magnetic moments of ternary $X_2X'Z$ compounds.

Systems (Type-I)	Lattice constant(Å)	Formation energy(eV)	Structure type	M ($\mu_B/f.u.$)
Mn ₂ YAl	6.52	-0.74	T _I	5.72
Mn ₂ ZrAl	6.15	-2.01	T _I	3.00
Mn ₂ NbAl	6.00 (6.005 ⁴⁶)	-1.56	T _I	2.00 (2.00 ⁴⁶)
Mn ₂ MoAl	5.90	-1.23	T _I	1.04
Mn ₂ TcAl	5.95	-1.94	T _{II}	0.04
Mn ₂ RuAl	5.95	-2.62	T _{II}	1.01
Mn ₂ RhAl	5.95	-2.08	T _{II}	1.86
Mn ₂ PdAl	6.05	-1.67	T _{II}	0.86
Mn ₂ AgAl	6.20	-0.29	T _{II}	0.31
Fe ₂ YAl	6.25	-0.47	T _I	1.95
Fe ₂ ZrAl	6.05	-1.96	T _I	0.91
Fe ₂ NbAl	5.90 (5.909 ⁴⁷)	-1.63	T _I	0.00
Fe ₂ MoAl	5.85	-0.77	T _I	0.82
Fe ₂ TcAl	5.85	-1.34	T _{II}	3.29
Fe ₂ RuAl	5.90	-1.97	T _{II}	5.20
Fe ₂ RhAl	5.90	-1.58	T _{II}	5.00
Fe ₂ PdAl	5.95	-1.25	T _{II}	4.84
Fe ₂ AgAl	6.05	0.25	T _{II}	4.75
Co ₂ YAl	6.20	-3.21	T _I	0.00
Co ₂ ZrAl	6.05	-4.32	T _I	1.00
Co ₂ NbAl	5.95	-3.31	T _I	2.00
Co ₂ MoAl	5.90	-2.36	T _I	2.84
Co ₂ TcAl	5.85	-3.14	T _I	3.91
Co ₂ RuAl	5.85	-3.38	T _{II}	3.87
Co ₂ RhAl	5.85	-2.84	T _{II}	3.37
Co ₂ PdAl	5.90	-2.56	T _{II}	3.04
Co ₂ AgAl	5.97	-1.28	T _{II}	2.77
Mn ₂ YSi	6.16	-1.01	T _I	3.02
Mn ₂ ZrSi	6.00 (6.004 ⁴⁸)	-2.42	T _I	2.00 ⁴⁸
Mn ₂ NbSi	5.87	-2.02	T _I	0.99
Mn ₂ MoSi	5.78	-1.61	T _I	0.00
Mn ₂ TcSi	5.83	-2.60	T _{II}	1.04
Mn ₂ RuSi	5.79	-3.10	T _{II}	2.00
Mn ₂ RhSi	5.81 (5.905 ⁴⁹)	-2.09	T _{II}	3.00 (3.00 ⁴⁹)
Mn ₂ PdSi	5.98	-1.39	T _{II}	0.95
Mn ₂ AgSi	6.11	0.14	T _{II}	0.59
Fe ₂ YSi	6.08	-0.87	T _I	0.96
Fe ₂ ZrSi	5.93 (5.899 ⁵⁰)	2.55	T _I	0.00
Fe ₂ NbSi	5.84	-1.58	T _I	0.97
Fe ₂ MoSi	5.78	-0.71	T _I	1.79
Fe ₂ TcSi	5.79	-1.88	T _{II}	3.78
Fe ₂ RuSi	5.78	-2.37	T _{II}	4.69
Fe ₂ RhSi	5.80	-1.59	T _{II}	4.90
Fe ₂ PdSi	5.88	-0.91	T _{II}	5.07
Fe ₂ AgSi	5.97	0.77	T _{II}	4.69
Co ₂ YSi	6.12	-3.32	T _I	1.00
Co ₂ ZrSi	5.99	-4.36	T _I	2.00
Co ₂ NbSi	5.87	-3.01	T _I	1.71
Co ₂ MoSi	5.78	-2.16	T _{II}	0.01
Co ₂ TcSi	5.72	-3.22	T _{II}	0.21
Co ₂ RuSi	5.74	-3.60	T _{II}	3.20
Co ₂ RhSi	5.76	-2.65	T _{II}	3.27
Co ₂ PdSi	5.79	-2.14	T _I	2.35
Co ₂ AgSi	5.83	-1.20	T _I	0.20

atoms hybridise the following way: first the atoms on symmetric sites (8c in the space group 225, 4c and 4d in space group-216) hybridise creating (i) 5 bonding d -hybrids (2 doubly-degenerate e_g and 3 triply degenerate t_{2g} hybrid orbitals) (ii) five non bonding hybrid d -orbitals (2 doubly-degenerate e_u and 3 triply degenerate t_{1u} hybrid orbitals)(Fig. 1(a) in Supplementary material). The bonding e_g and t_{2g} orbitals, having tetrahedral symmetry, can only hybridise with d -orbitals of the remaining transition metal atom. Thus, ultimately we are left with five bonding and five anti-bonding states which are non-transforming with the u representation^{4,57} and can not couple with d -orbitals of the remaining transition atom (Fig. 1(b) in Supplementary material).

In case of a half-metal there is an energy gap in one spin-channel, where the Fermi-energy is pinned in. The position of the Fermi-level in a spin-channel where the half-metallic gap is situated, determines which Slater-Pauling rule the material follows as the number of states in that particular spin-channel below the Fermi-level is always fixed and any extra electron would be placed in unoccupied states of other spin-channel. In this paper we use the convention that if $N_V > 24$, the spin channel where the half-metallic gap is, will be considered the minority spin channel. Accordingly, from Fig. 1, Supplementary material, it is clear that position of E_F in the minority spin-channel would lead to the half-metals following different Slater-Pauling rules. If E_F is situated between t_{1u} and t_{2g} states, it would follow $M = |N_V - 18|$ rule. If the position of Fermi-energy is between t_{1u} and e_u states, the compound would follow $M = |N_V - 24|$ rule. Simple difference in electron count in both spin-channel leads us to this conclusion.

In Figs. 3- 8 we present the spin-polarised total and atom projected densities of states of all $X_2X'Z$ compounds considered in this work in their respective ground state structures. In the following we discuss them series-wise.

a. $Mn_2X'Z$ compounds

The densities of states for compounds of $Mn_2X'Al$ ($Mn_2X'Si$) series with T_I and T_{II} structures are shown, respectively, In Fig 3.(a) and Fig 4.(a) (Fig 3.(b) and Fig 4.(b)). We find several features common to either the compounds with same structure type or even across the structure types: (a) for compounds in T_I structure and with possible half-metallic gaps, the gaps are flanked by Mn d -states, while for compounds in T_{II} structure, the contributions from Mn and X' are significant; both consistent with the generalised hybridisation picture described above, (b) across the structures, as the atomic number increases, the contributions from X' move gradually towards lower energies, (c) as long as structure types are same, the features in the densities of states of compounds from the two different series are very similar when N_V are same. This is reflected more in compounds with structure T_I . For example, Mn_2NbAl and Mn_2ZrSi both are half-metallic with $N_V=22$. Mn_2ZrAl and

Mn_2YSi , Mn_2MoAl and Mn_2NbSi too have similar features in their densities of states. On the other hand, Mn_2MoSi and Mn_2TcAl , both are with $N_V=24$, yet have completely different features in their densities of states as the ground state structures are different.

In order to identify half-metals and understand their origin as N_V changes continuously, we now focus on the densities of states of the compounds in the two series systematically. We find that for compounds crystallising in T_I the origin of the gap in majority spin channel is due to the splitting of non-bonding t_{1u} and e_u states arising out of hybridisations between the Mn atoms. For Mn_2ZrAl and Mn_2YSi the separation between t_{1u} and e_u states are not enough to extend the gap cutting through the Fermi-level to make these compounds half-metallic. Thus, inspite of their magnetic moments being integer or near integer, these compounds are not half-metals. As we go from Mn_2ZrAl (Mn_2YSi) to Mn_2NbAl (Mn_2ZrSi), the extra electron is accommodated in one of the three t_{1u} states in the majority band opening a half-metallic gap. In Mn_2MoAl (Mn_2NbSi) the extra electron is accommodated in one of the vacant t_{1u} or in the e_g states in the majority bands, thus producing high spin polarisation but destroying the half-metallicity as these states cut through the Fermi levels. Once again, inspite of having near integer moments, these two compounds at best can be considered near half-metals with Mn_2NbSi having a spin polarisation over 90%. Mn_2MoSi , with $N_V=24$, has same occupancy in both spin bands leading to zero magnetic moment, in conformation with the Slater-Pauling rule. However, inspite of Mn_2TcAl having $N_V=24$ too, the electronic structure is different from that of Mn_2MoSi as the former crystallises in T_{II} structure. Though the moment is nearly zero in Mn_2TcAl (like Mn_2MoSi) it has a large spin polarisation of 94%. This is because unlike Mn_2MoSi , it has a near half-metallic gap in the majority spin band arising out of the separation of bonding t_{2g} and non-bonding e_u states across the Fermi level. This, in fact, is part of the general features observed in the electronic structure of the compounds with T_{II} structure. In case of these compounds the bonding t_{2g} hybrid orbitals, originating from all the transition metal atoms and the non-bonding t_{1u} hybrids due to Mn and X' atoms lie extremely close; same happens for anti-bonding e_g and non-bonding e_u states. Throughout the $Mn_2X'Z$ series with T_{II} structure, we find that the position of the gap and spin polarisation is determined by this.

Thus, in $Mn_2X'Z$ series we found three true half-metals (Mn_2NbAl , Mn_2ZrSi and Mn_2RhSi), four near half-metals *i.e.* materials with high spin polarisation (greater than 90%) (Mn_2TcAl , Mn_2RuAl , Mn_2NbSi , Mn_2RuSi). Out of the three true half-metals, Mn_2RhSi has also been found to be a potential thermoelectric material⁴⁹. On the other hand, near half-metal Mn_2TcAl with it's high spin polarisation and near zero magnetic moment is a potential compensated ferrimagnet. It may be noted that Mn_3Al in DO_3 structure is a well known compensated ferrimagnet⁵⁸ and that Mn_2TcAl is isoelectronic to it (derived by replacing one Mn with Tc), implying that

the physical properties of magnetic Heusler compounds obtained by replacing one $3d$ element with a $4d$ may depend solely on N_V . We find a signature of this when we compare Mn_2YAl and Mn_2ScAl . Our calculations show that Mn_2YAl is not a half-metal at all, neither does it have a significant spin polarisation. However, it has exceptionally large magnetic moment exactly like Mn_2ScAl , which is isoelectronic.

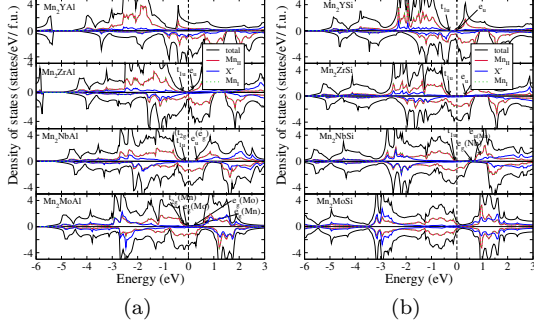


FIG. 3: Spin polarized total and atom-projected densities of states for (a) $Mn_2X'Al$ and (b) $Mn_2X'Si$ ($X' = Y, Zr, Nb, Mo$) compounds. The ground states of these compounds are Type-I.

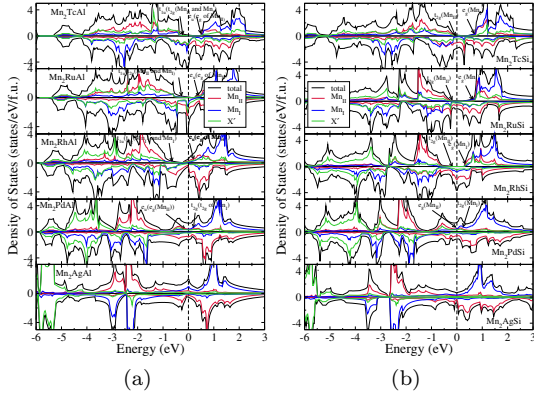


FIG. 4: Spin polarized total and atom-projected densities of states for (a) $Mn_2X'Al$ and (b) $Mn_2X'Si$ ($X' = Y, Zr, Nb, Mo$) compounds. The ground states of these compounds are Type-II.

b. $Fe_2X'Z$ compounds

Atom and spin resolved densities of states of $Fe_2X'Z$ series are presented in the Fig 5 and Fig 6. Fig 5.(a) and Fig 5.(b) (Fig 6.(a) and Fig 6.(b)) are the densities of states for compounds with structure type $T_I(T_{II})$. We find substantial similarities between $Fe_2X'Z$ and $Mn_2X'Z$ as far as some of the general features in the electronic structures are concerned. Like in $Mn_2X'Z$ series, the main contributions to densities of states for compounds in $Fe_2X'Z$ near Fermi levels come from the Fe atoms in case of compounds with structure

T_I whereas in case of compounds with T_{II} structure, the main contributions come from the tetrahedrally co-ordinated Fe and X' atoms. We also find that with increasing atomic number the X' d - states lie deeper into the valence band, a feature similar to the $Mn_2X'Z$ series. The major difference, however, between the compounds in two series, is that none of the 18 compounds in Fe_2X' series is found to be half-metallic. This difference originates from the fact that the Fe states are more delocalised as compared to Mn states. As a result, often the Fe states or the ones with hybridisations with Fe atoms, extend into the unoccupied part, leaving no possibility of opening up of a half-metallic gap. However, in almost all compounds, there is either a pseudo gap in the occupied part of one spin channel and a gap like valley cutting through the Fermi level in the other. The trends in the features of the electronic structures as one goes through the compounds in a series and with a given crystal structure, are same across the Al and Si series. The electronic structures are very similar if N_V is same. For compounds with structure type T_I , the electronic structure near the Fermi level is contributed mostly by the t_{2g} and e_g Fe states in occupied and unoccupied parts respectively. We find the only near half-metal in Fe-series compounds to be Fe_2NbSi with spin polarisation 95% crystallising in T_I structure. The compound right before Fe_2NbSi in the series is Fe_2ZrSi which has 24 valence electrons and turns out to be a non-magnetic semiconductor. It is interesting to note that unlike $Mn_2X'Z$, the changes in the electronic structure of $Fe_2X'Z$ compounds, when N_V changes from 23 to 24 are drastic. In the Mn-series, the changes in electronic structures between Mn_2NbAl ($N_V=23$) and Mn_2MoAl ($N_V=24$) bore a continuity while the changes from Fe_2ZrAl (Fe_2YSi) to Fe_2NbAl (Fe_2ZrSi) are sharp and substantial. The changes from Fe_2NbAl (Fe_2ZrSi) to Fe_2MoAl (Fe_2NbSi) again are systematic, following a trend. The extra electron in Fe_2MoAl (in comparison to Fe_2ZrAl) is accommodated in the spin-up band, which reflects in a pseudo gap inside the occupied part of spin up channel. The semiconducting gap of Fe_2NbAl in the spin down channel would have been intact if the hybridisations near the Fermi level wouldn't have changed upon replacement of Nb with Mo. The hybridisations of Mo and Fe states near the Fermi level produce a valley cutting through the Fermi level, reducing the magnetic moment significantly from the Slater-Pauling predicted value, bringing down the spin polarisation as well. The semiconducting gap of spin down channel in Fe_2ZrSi nearly survives in Fe_2NbSi as the Nb e_g and Fe t_{2g} hybridisations near Fermi level are weak as compared to Fe_2MoAl . For the compounds with structure type T_{II} , the proximity of d states of Fe and X' mix the states substantially in both spin channels, leaving little possibility of a semiconducting gap in any of the spin channels.

c. $Co_2X'Z$ compounds

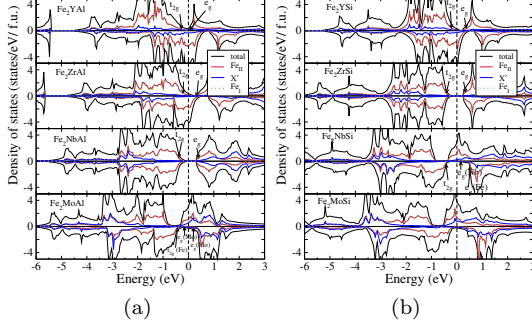


FIG. 5: Spin polarized total and atom-projected densities of states for (a) $\text{Fe}_2\text{X}'\text{Al}$ and (b) $\text{Fe}_2\text{X}'\text{Si}$ ($\text{X}' = \text{Y, Zr, Nb, Mo}$) compounds. The ground states of these compounds are Type-I.

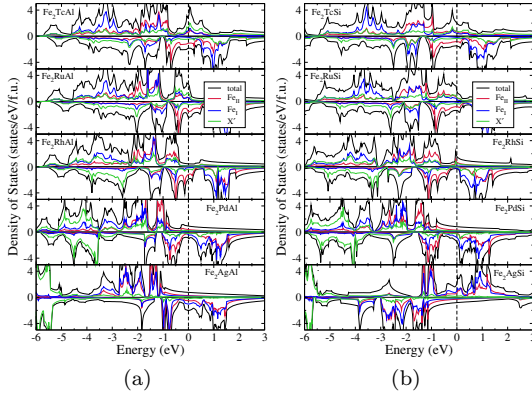


FIG. 6: Spin polarized total and atom-projected densities of states for (a) $\text{Fe}_2\text{X}'\text{Al}$ and (b) $\text{Fe}_2\text{X}'\text{Si}$ ($\text{X}' = \text{Y, Zr, Nb, Mo}$) compounds. The ground states of these compounds are Type-II.

In Figs 7 - 8 we show the total and partial densities of states of $\text{Co}_2\text{X}'\text{Z}$ compounds. Like observed in cases of Mn_2 and Fe_2 based compounds, the Co_2 based compounds with structure T_I have Co states dominating the features near the half-metallic gaps for half-metals. We find more half-metals with 100% spin polarisations among $\text{Co}_2\text{X}'\text{Z}$ compounds in comparison to compounds in other two series. All the half-metals in Co_2 -compounds are with T_I structure, arising because of the Co states, localised more in comparison to Mn or Fe in Mn_2 and Fe_2 based compounds respectively. This feature is also seen in the more familiar $\text{Co}_2\text{X}'\text{Z}$ compounds with X' a 3d element^{4,59,60}. The Co-based compounds studied in the present work have N_V greater than or equal to 24. Thus the half-metallic gaps are found in the spin down channels. In Fig 7.(a) and Fig 7.(b) we see that the main contributions to densities of states comes from $\text{Co-}t_{2g}$ or $\text{Co-}t_{1u}$ below the Fermi-level and from $\text{Co-}e_g$ or $\text{Co-}e_u$ above the Fermi-level in both $\text{Co}_2\text{X}'\text{Al}$ and $\text{Co}_2\text{X}'\text{Si}$ series. Co_2YAl , having $N_\text{V}=24$, is a non-magnetic compound where each spin band has exactly 12 electrons. In Co_2ZrAl - Co_2NbAl (Co_2YSi -

Co_2ZrSi) minority spin channel have 12 electrons and the extra electrons are fully accommodated in the majority spin channel opening the gap in minority spin channel. In Co_2MoAl (Co_2NbSi) the extra electron is not fully accommodated in the next e_g band in spin up channel, instead it is shared by both the spin channels, thus destroying the half-metallicity. In Co_2TcAl the extra electron, as expected, is not placed totally in the anti-bonding e_g states in spin up channel and there is considerable mixing of Co and Tc e_g states near Fermi level leaving little chance of half-metallicity. Co_2PdSi and Co_2AgSi , the other two compounds with T_I structure have different hybridisation pattern where delocalised Pd and Ag states hybridise considerably with Co states near Fermi level, leading them to behave like normal metals.

The compounds with T_II structures have significant hybridisations between Co and X' states in both spin channels and thus there is no possible half-metals with this crystal structure. Like the Mn_2 and Fe_2 series, this is an artefact of the atomic arrangement in T_II structure. Thus, in $\text{Co}_2\text{X}'\text{Z}$ series we find four half-metals, Co_2ZrAl , Co_2NbAl , Co_2ZrSi and Co_2NbSi , having 100% spin polarisation.

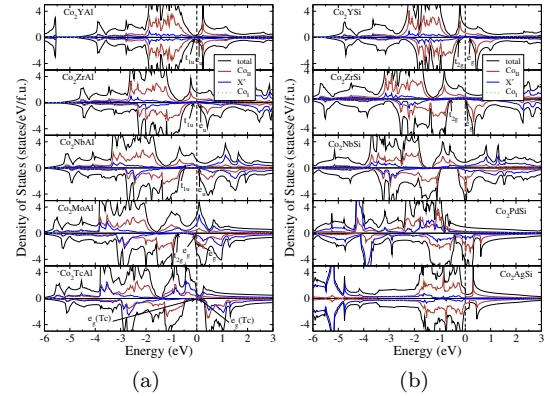


FIG. 7: Spin polarized total and atom-projected densities of states for (a) $\text{Co}_2\text{X}'\text{Al}$ and (b) $\text{Co}_2\text{X}'\text{Si}$ ($\text{X}' = \text{Y, Zr, Nb, Mo}$) compounds. The ground states of these compounds are Type-I.

D. Trends in the local magnetic moments

In Tables II to VII we present the total and site projected magnetic moments along with the spin polarisations for all the compounds considered here. We try to understand the magnetic structures, the contributions of each transition metal atom towards the total moments, and the trends in variations of the atomic moments across series and structures. We also intend to relate such trends with the trends in the electronic structures discussed in previous sub-section.

The 3d elements contribute most towards the magnetic structure and the overall magnetisation in all the com-

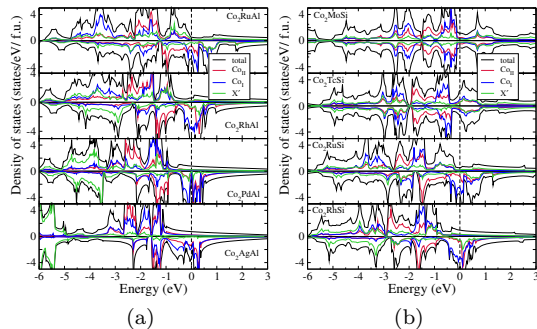


FIG. 8: Spin polarized total and atom-projected densities of states for (a) $\text{Co}_2\text{X}'\text{Al}$ and (b) $\text{Co}_2\text{X}'\text{Si}$ ($\text{X}' = \text{Y, Zr, Nb, Mo}$) compounds. The ground states of these compounds are Type-II.

pounds studied here. This is a reflection of the facts that the electronic structures of these compounds evolve around the electronic structures of the $3d$ constituents throughout the series. For compounds with structure type T_I we find that the moments of the $3d$ constituents are very close across the corresponding Al and Si series, the only exceptions being Co_2MoAl and Co_2NbSi . For compounds with structure type T_II , there is no such trend. For Mn_2 -compounds, Mn moments differ substantially between the compounds in Al series and those in Si series. The moments of Mn_I , the Mn atoms at the $4c$ sites, are considerably reduced in the compounds of Si series, as compared to those in the Al series. The trend is not so in cases of the Fe- and Co-series, except few cases like Fe_2RuAl - Fe_2TcSi and Co_2RuAl - Co_2TcSi pairs.

The moments of Mn atoms in both $\text{Mn}_2\text{X}'\text{Al}$ and $\text{Mn}_2\text{X}'\text{Si}$ series decrease with N_V for compounds with structure type T_I . The opening of the gap in the spin up band and subsequent increase in the electrons in the spin down band, as explained in the previous sub-section, is responsible for such trend. For compounds with structure type T_II , the two Mn atoms are ferrimagnetically coupled due to they being nearest neighbours. We find that in both Al- and Si-series, the moment of Mn_II , the Mn atom at the $4a$ sites, is much robust and increases gradually with N_V . This is because of the fact that the Mn_II spin up band is nearly full with a near gap close to the Fermi level while the spin down band gradually becomes empty. The Mn_I atom, on the other hand, hybridises well with X' as they occupy symmetric positions and thus loses the robustness in its moment. The re-distributions of states among the spin bands due to the hybridisations of Mn and X' d -orbitals are more prominent in the compounds of the Si-series which is responsible for the substantial reductions in the Mn_I moments.

The drastic changes in the electronic structures of Fe_2 -compounds crystallising in T_I structure when N_V is equal to or greater than 24 reflect in the Fe moments. The Fe moment decreases significantly from Fe_2YAl to Fe_2ZrAl . The extra electron in Fe_2ZrAl occupies the spin down band of Fe reducing the moment. The moment starts to

TABLE II: Total and atomic magnetic moment of $\text{Mn}_2\text{X}'\text{Al}$ systems in $\mu_B/f.u.$. N_V is the number of valence electron of the systems. M is the total moment and M_i is the moment of constituent i .

Systems(T_I)	N_V	M	M_{MnI}	M_{MnII}	$M_{\text{X}'}$	M_{Al}	P(%)
Mn_2YAl	20	5.72	2.99	2.99	-0.13	-0.07	39
Mn_2ZrAl	21	3.00	1.73	1.73	-0.34	-0.05	74
Mn_2NbAl	22	2.00	1.21	1.21	-0.36	-0.03	100
Mn_2MoAl	23	1.04	0.68	0.68	-0.31	-0.01	88

Systems(T_II)	N_V	M	M_{MnI}	$M_{\text{X}'}$	M_{MnII}	M_{Al}	P(%)
Mn_2TcAl	24	0.04	-2.35	-0.37	2.75	0.03	94
Mn_2RuAl	25	1.01	-2.18	0.06	3.07	0.02	96
Mn_2RhAl	26	1.86	-1.84	0.34	3.26	0.01	6
Mn_2PdAl	27	0.86	-2.80	0.13	3.45	0.01	4
Mn_2AgAl	28	0.31	-3.12	0.03	3.40	0.01	59

pick up after N_V is beyond 24. The extra electron now starts to occupy the Fe spin up band primarily. This explains the trends in the $\text{Fe}_2\text{X}'\text{Si}$ compounds. Like observed in the Mn-series, Fe_II moment in compounds with structure type T_II is robust. Although the magnetic interaction between Fe atoms is ferromagnetic, substantial states in Fe_I close to Fermi level, an artefact of hybridisations with X' , reduces its moment in comparison to Fe_II .

In contrast, Co moment in $\text{Co}_2\text{X}'\text{Z}$ compounds with structure type T_I increases with N_V , the only exception being Co_2NbSi where the Co moment decreases in comparison to that in Co_2ZrSi . The electronic structures provide clue to this trend. As the extra electrons available with increasing N_V are gradually accommodated primarily in the spin up bands, the moment increases. In case of Co_2NbSi , the extra electron available with respect to Co_2ZrSi is shared between both spin bands, thus departing from the general trend. Same trend is seen Co_II moment in compounds with structure type T_II . The Co_I moments, though reduced in comparison to those of Co_II , the reduction is less substantial in comparison to Mn_2 - and Fe_2 -compounds. The extra electron available as N_V increases is accommodated primarily in the spin down band, reducing the moment of Co_II . The moment of Co_I , on the other hand, hardly changes from compound to compound.

In all the compounds, the X' atom contributes to the overall magnetic moment, mostly for structure type T_II . The greater hybridisation with the $3d$ element, as a consequence of geometry, is responsible for this. Al and Si atoms have vanishingly small contributions in all cases.

E. Exchange interactions and Curie temperature

In Fig 9 and 10 we show the variations of Curie temperatures with changes in the valance electron number for $\text{X}_2\text{X}'\text{Al}$ ($\text{X} = \text{Mn, Fe, Co}$) and $\text{X}_2\text{X}'\text{Si}$ ($\text{X} = \text{Mn, Fe, Co}$) series respectively. Our results show that the variations in the Curie temperatures can be classified in two

TABLE III: otal and atomic magnetic moment of $Mn_2X'Si$ systems in $\mu_B/f.u.$. N_V is the number of valence electron of the systems. M is the total moment and M_i is the moment of constituent i..

Systems(T_I)	N_V	M	M_{MnI}	M_{MnII}	$M_{X'}$	M_{Si}	$P(\%)$
Mn_2YSi	21	3.02	1.64	1.64	-0.10	-0.07	66
Mn_2ZrSi	22	2.00	1.12	1.12	-0.20	-0.04	100
Mn_2NbSi	23	0.99	0.59	0.59	-0.17	-0.02	93
Mn_2MoSi	24	-0.00	-0.00	-0.00	0.00	0.00	0

Systems(T_{II})	N_V	M	M_{MnI}	$M_{X'}$	M_{MnII}	M_{Si}	$P(\%)$
Mn_2TcSi	25	1.04	-1.38	-0.30	2.63	0.05	87
Mn_2RuSi	26	2.00	-0.85	0.07	2.70	0.03	91
Mn_2RhSi	27	3.00	-0.44	0.30	3.04	0.02	100
Mn_2PdSi	28	0.95	-2.59	0.08	3.37	0.04	13
Mn_2AgSi	29	0.59	-2.88	0.02	3.39	0.04	15

TABLE IV: Total and atomic magnetic moment of $Fe_2X'Al$ systems in $\mu_B/f.u.$. N_V is the number of valence electron of the systems. M is the total moment and M_i is the moment of constituent i..

Systems(T_I)	N_V	M	M_{FeI}	M_{FeII}	$M_{X'}$	M_{Al}	$P(\%)$
Fe_2YAl	22	1.95	1.17	1.17	-0.18	-0.04	89
Fe_2ZrAl	23	0.91	0.54	0.54	-0.12	-0.01	85
Fe_2NbAl	24	0.00	0.00	0.00	0.00	0.00	0
Fe_2MoAl	25	0.82	0.48	0.48	-0.07	-0.01	84

Systems(T_{II})	N_V	M	M_{FeI}	$M_{X'}$	M_{FeII}	M_{Al}	$P(\%)$
Fe_2TcAl	26	3.29	1.51	-0.26	2.06	-0.01	22
Fe_2RuAl	27	5.20	2.23	0.49	2.59	-0.03	2
Fe_2RhAl	28	5.00	1.98	0.39	2.77	-0.04	62
Fe_2PdAl	29	4.84	2.00	0.14	2.78	-0.04	1
Fe_2AgAl	30	4.75	2.19	-0.00	2.63	-0.04	44

distinct regions based on structure types. Though the region-wise variations are not uniform it gives a qualitative idea of dependence of Curie temperatures on the ordering of the atoms. we analyse the trends in the variations of Curie temperatures by inspecting the variations of different effective exchange parameters $J_{\mu\nu}^{eff}$ (Fig.11 and Fig.12 of supplementary material) being given as $J_{\mu\nu}^{eff} = \sum_j J_{\mu\nu}^{0j}$; 0 fixed on μ sub-lattice and j runs over ν sub-lattice.

For $Mn_2X'Z$ compounds with structure type T_I , the Mn-Mn ferromagnetic interactions decide the variations in the Curie temperature T_c . This is true for $Fe_2X'Z$ and $Co_2X'Z$ series with compounds crystallising in T_I . The highest T_c is thus obtained for Mn_2ZrAl and Mn_2ZrSi for Mn-series, Fe_2YAl and Fe_2MoSi for Fe-series, Co_2NbAl and Co_2ZrSi for Co-series. Among them, the Co-compounds have the highest T_c and the Fe-compounds have the lowest T_c . This trend can be understood from the higher J^{eff} for Co-compounds and relatively lower ones in Fe-compounds. In case of Co-compounds, along with Co-Co, Co- X' ferromagnetic interactions too play a significant role in deciding T_c . We find that both J^{eff} are maximum for $N_V=26$ across the Z series for Co-compounds. This can be attributed to the changes

TABLE V: Total and atomic magnetic moment of $Fe_2X'Si$ systems in $\mu_B/f.u.$. N_V is the number of valence electron of the systems. M is the total moment and M_i is the moment of constituent i..

Systems(T_I)	N_V	M	M_{FeI}	M_{FeII}	$M_{X'}$	M_{Si}	$P(\%)$
Fe_2YSi	23	0.96	0.54	0.53	-0.05	-0.02	89
Fe_2ZrSi	24	0.00	0.00	0.00	-0.00	-0.00	0
Fe_2NbSi	25	0.97	0.60	0.60	-0.14	-0.01	95
Fe_2MoSi	26	1.79	0.96	0.96	-0.05	-0.01	88

Systems(T_{II})	N_V	M	M_{FeI}	$M_{X'}$	M_{FeII}	M_{Si}	$P(\%)$
Fe_2TcSi	27	3.78	1.37	-0.05	2.43	0.01	16
Fe_2RuSi	28	4.69	1.65	0.34	2.74	-0.02	8
Fe_2RhSi	29	4.90	1.72	0.38	2.85	-0.03	71
Fe_2PdSi	30	5.07	2.08	0.18	2.79	-0.02	31
Fe_2AgSi	31	4.69	2.07	0.00	2.62	-0.02	46

TABLE VI: Total and atomic magnetic moment of $Co_2X'Al$ systems in $\mu_B/f.u.$. N_V is the number of valence electron of the systems. M is the total moment and M_i is the moment of constituent i..

Systems(T_I)	N_V	M	M_{CoI}	M_{CoII}	$M_{X'}$	M_{Al}	$P(\%)$
Co_2YAl	24	0.00	0.00	0.00	0.00	0.00	0
Co_2ZrAl	25	1.00	0.59	0.59	-0.10	-0.00	100
Co_2NbAl	26	2.00	1.02	1.02	0.01	0.00	100
Co_2MoAl	27	2.84	1.19	1.19	0.47	-0.01	4
Co_2TcAl	28	3.91	1.36	1.36	1.25	-0.03	56

Systems(T_{II})	N_V	M	M_{CoI}	$M_{X'}$	M_{CoII}	M_{Al}	$P(\%)$
Co_2RuAl	29	3.87	1.32	0.70	1.94	-0.01	69
Co_2RhAl	30	3.37	1.31	0.39	1.80	-0.02	79
Co_2PdAl	31	3.04	1.46	0.04	1.63	-0.01	54
Co_2AgAl	32	2.77	1.34	-0.02	1.56	-0.02	64

in the behaviour of the Exchange average, the average of exchange energies associated with low temperature spin excitations. This variation in the Exchange average is related to the availability of spin down states below Fermi level. A gap in the spin down bands starting below Fermi level and extending beyond would lead to a larger value of Exchange average and consequently a larger Curie temperature⁶¹. This, exactly, is happening for Co-compounds considered here. The same explanation can be used for Mn_2 - compounds. The absence of such clear gaps around Fermi level of Fe-compounds imply that this argument cannot be used and thus the trends in variations of T_c is qualitatively different.

The dominant exchange interactions for compounds with structure type T_{II} are $Mn_I(Co_I,Fe_I)-Mn_{II}(Co_{II},Fe_{II})$, $Mn_{II}-Mn_{II}$ ($Co_{II}-Co_{II}$, $Fe_{II}-Fe_{II}$) and $Mn_{II}-X'(Co_{II}-X', Fe_{II}-X')$. For Mn-compounds, the Mn_I-Mn_{II} interactions are strongly antiferromagnetic while the interactions between the 3d magnetic atoms are ferromagnetic for compounds in other two series. In case of Mn-compounds, the T_c for Si-series is generally less than Al-series. The reason is that in the compounds in Si series there are competing antiferromagnetic and ferromagnetic interactions with the ferromagnetic ones

TABLE VII: Total and atomic magnetic moment of $\text{Co}_2\text{X}'\text{Al}$ systems in $\mu_B/f.u.$. N_V is the number of valence electron of the systems. M is the total moment and M_i is the moment of constituent i .

Systems(T_I)	N_V	M	M_{CoI}	M_{CoII}	$M_{X'}$	M_{Si}	$P(\%)$
Co_2YSi	25	1.00	0.58	0.58	-0.12	0.01	100
Co_2ZrSi	26	2.00	1.04	1.04	-0.07	0.04	100
Co_2NbSi	27	1.71	0.83	0.83	0.04	0.03	72
Systems(T_{II})	N_V	M	M_{CoI}	$M_{X'}$	M_{CoII}	M_{Si}	$P(\%)$
Co_2MoSi	28	0.01	0.02	-0.00	-0.01	-0.00	0
Co_2TcSi	29	0.21	0.04	0.02	0.14	0.00	22
Co_2RuSi	30	3.20	1.12	0.48	1.67	-0.01	74
Co_2RhSi	31	3.27	1.34	0.44	1.56	-0.01	65
Systems(T_I)	N_V	M	M_{CoI}	M_{CoII}	$M_{X'}$	M_{Si}	$P(\%)$
Co_2PdSi	32	2.35	1.17	1.17	0.11	-0.04	69
Co_2AgSi	33	0.20	0.12	0.12	-0.01	-0.01	18

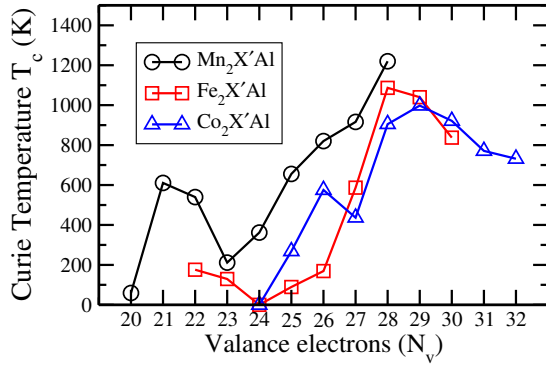


FIG. 9: Variations in the Calculated Curie temperature with total number of valence electron for $\text{X}_2\text{X}'\text{Al}$ ($X = \text{Mn, Fe, Co}$) series.

coming from $\text{Mn}_{II}\text{-Mn}_{II}$ and $\text{Mn}_{II}\text{-X}'$ interactions. The variations in the T_c for compounds in each series are controlled by the variations in the various dominant J^{eff} .

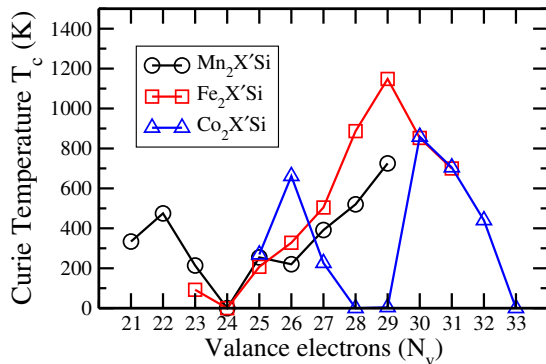


FIG. 10: Variations in the calculated Curie temperature with total number of valence electron for $\text{X}_2\text{X}'\text{Si}$ series.

F. Trends in the electronic properties upon replacing a 3d X' constituent with an isoelectronic 4d element

There is lot more half-metals and SGS discovered among $\text{X}_2\text{X}'\text{Z}$ Heusler compounds with all transition metal atoms from 3d series. It would, thus, be interesting and important to understand the impact of replacing a 3d X' constituent with an isoelectronic 4d element. A comparison into the half-metallic aspects of the isoelectronic compounds which are either half-metals or near half-metals with high spin polarisation in either or both series (one with X' a 3d element and another with X' an isoelectronic 4d element) would shed light to the following: (a) whether electronic properties like half-metallicity primarily depends on N_V and not on whether X' is a 3d element or a 4d element and (b) if not, then which are the possible factors that can explain the comparative trends in the isoelectronic compounds where in each case a 3d X' is replaced with its isoelectronic 4d counterpart. Addressing this issue would help in prediction and design of new half-metals.

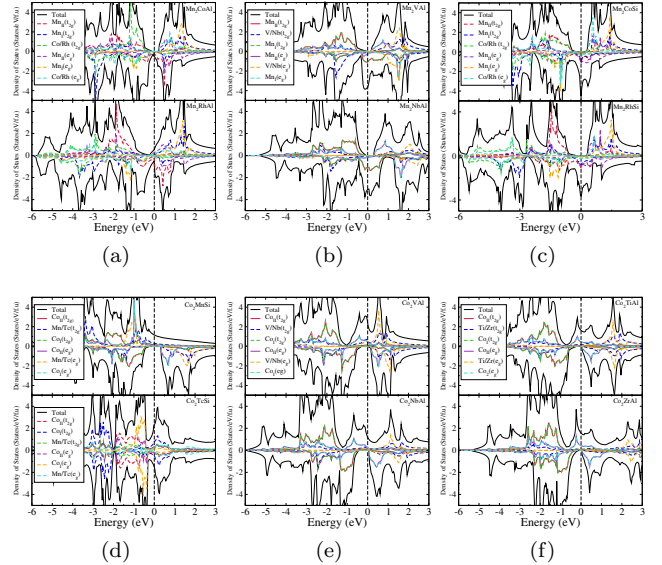


FIG. 11: Spin polarized total and atom-projected densities of states for pairs of isoelectronic compounds (a) $\text{Mn}_2\text{CoAl-Mn}_2\text{RuAl}$ (b) $\text{Mn}_2\text{VAl-Mn}_2\text{NbAl}$ (c) $\text{Mn}_2\text{CoSi-Mn}_2\text{RhSi}$ (d) $\text{Co}_2\text{MnSi-Co}_2\text{TcSi}$ (e) $\text{Co}_2\text{VAl-Co}_2\text{NbAl}$ and (f) $\text{Co}_2\text{TiAl-Co}_2\text{ZrAl}$.

In Table I of supplementary material, the structural, magnetic and electronic properties associated with half-metallicity of $\text{X}_2\text{X}'\text{Z}$ ($X = \text{Co, Mn, Fe}$; X' = an element with 3d electrons; $Z = \text{Al, Si}$) obtained from various existing resources are tabulated. Focusing solely on the compounds with integer or near integer magnetic moments and spin polarisation equal to or close to 100%, we find that Mn_2VAl and Mn_2CoSi are half-metals, Mn_2TiSi and Mn_2FeAl are near half-metals while Mn_2CoAl is a SGS; Fe_2MnSi is a half-metal while Fe_2CrAl and Fe_2CrSi are near half-metals; Co_2TiAl , Co_2CrAl , Co_2ScSi and

Co_2CrSi are half-metals while Co_2VAl is a near half-metal. For each of these compounds, we look at the spin polarisations of the isoelectronic counterpart in the series with X' a $4d$ element and find the following: (i) Mn_2VAl - Mn_2NbAl and Mn_2CoSi - Mn_2RhSi pairs are half-metals, Mn_2FeAl - Mn_2RuAl pairs are near half-metals with high spin polarisation, Mn_2TiSi is a near half metal while isoelectronic Mn_2ZrSi is a half-metal, Mn_2CoAl in structure type T_{II} is a SGS while Mn_2RhAl is an ordinary metal, (ii) Fe_2MoAl and Fe_2MoSi are ordinary metals while their isoelectronic counterparts with X' a $3d$ element, Fe_2CrAl and Fe_2CrSi , respectively are compounds with high spin polarisations. Fe_2TcSi is an ordinary metal while Fe_2MnSi is a half-metal, (iii) Co_2TiAl - Co_2ZrAl and Co_2ScSi - Co_2YSi are half-metal pairs, Co_2CrAl and Co_2MnSi are half-metals while their isoelectronic counterparts Co_2MoAl and Co_2TcAl , respectively, are ordinary metals with low spin polarisations, Co_2VAl is a near half metal while Co_2NbAl is a half metal. Co_2TiSi is an ordinary metal while Co_2ZrSi is a half-metal. Co_2CrSi is a half-metal while Co_2MoSi is a non-magnetic material.

In order to understand the trend observed, we take recourse to the comparisons of the electronic structures of each pairs of compounds considered above. In Fig. 11 and in Figs. 13-17 of supplementary material we show the total and partial densities of states of some of the pairs. In cases of Mn_2CoSi - Mn_2RhSi and Mn_2VAl - Mn_2NbAl pairs (Fig. 11 (b),(c)), we find that the electronic structures of a given pair are near identical around the Fermi levels. In cases of inverse Heusler (structure type T_{II}) Mn_2CoSi and Mn_2RhSi , the half-metallic gaps are artefacts of the separation of the t_{2g} and e_g spin up states. However, there is a difference between the contributors to these states between the two compounds: In Mn_2RhSi , the states bordering the gap are primarily Mn_{I} t_{2g} and a hybridised Mn_{II} -Rh e_g while in Mn_2CoSi , the t_{2g} states too are hybridised Mn_{I} -Co. In case of the pair Mn_2VAl - Mn_2NbAl , both in regular Heusler structure (structure type T_{I}), the electronic structures in the majority band is identical-the half-metallic gap being flanked by Mn states only. In Fig. 13 of supplementary material, we show the densities of states of the pair Mn_2TiSi - Mn_2ZrSi , the later is a half-metal while the former is a near half-metal with integer moment and above 90% spin polarisation (Table I, supplementary material). The densities of states reveal that the difference in the electronic properties originates from the positions of the t_{2g} and e_g states flanking the half-metallic gap; in Mn_2TiSi , the position of the top of the t_{2g} spin up bands in the occupied part coming from the Mn atoms cut through the Fermi level while this is not so in case of Mn_2ZrSi . The little trace of densities of states at the Fermi level reduces the spin polarisation in Mn_2TiSi . The striking difference in electronic properties in the context of half-metallicity is observed in the pair Mn_2CoAl - Mn_2RhAl with the former being a SGS and both are of structure type T_{II} . A close inspection into the densities of states (Fig. 11 (a)), however, reveals that the electronic structures of the two compounds are not so different from each other-in both compounds top of the

valence band and bottom of the conduction band touch each other forming zero gap in the spin down band. A difference occurs in the spin up bands. In Mn_2CoAl , there is a clear half-metallic gap with the top of the valence band having contributions from Mn_{II} and Co t_{2g} states and the bottom of the conduction band having contributions from the e_g states of the same pair of atoms. In Mn_2RhAl , we find another zero gap in the spin up bands, however, not at the fermi level but inside the occupied part of the spectrum. The t_{2g} and e_g bands in this case are more delocalised, possibly due to hybridisations with more delocalised $4d$ states of Rh as compared to $3d$ states of Co, thus, diminishing chances of getting SGS or half-metallic properties in this compound.

The origin of different properties in Fe_2MnSi - Fe_2TcSi pair can be traced to the structures they crystallise in: the former in T_{I} and the later in T_{II} . In Fig. 14 of supplementary material, we compare the densities of states of two compounds. The half-metallic behaviour of Fe_2MnSi stems from the unavailability of spin down states on either side of Fermi level with the gap being flanked by Fe t and e states. In Fe_2TcSi , the T_{II} structure leaves no such scope as there is substantial hybridisations between Fe and Tc states across the Fermi level. The pairs Fe_2CrAl - Fe_2MoAl and Fe_2CrSi - Fe_2MoSi all crystallise in same structure (type T_{I}) but their spin polarisations differ significantly. However, the densities of states of each pair of compounds are qualitatively similar. The highlights of the electronic structure in both Fe_2CrAl ⁶² and Fe_2MoAl are a pseudogap in the spin up band and a gap cutting through the Fermi level in the spin down band, although in case of Fe_2MoAl , it is more like a pseudo gap reducing it's spin polarisation. This difference in the electronic structure once again stems from the availability of states near and at Fermi level in case of Fe_2MoAl , presumably because of the hybridisations of Fe with delocalised Mo states. Similar differences explain the differences in spin polarisations of Fe_2CrSi and Fe_2MoSi .

In Fig. 11 (d)-(f), we show the densities of states for three pairs of Co_2 -compounds. The Co_2TiAl - Co_2ZrAl pair is a half-metal one, in Co_2VAl - Co_2NbAl pair, the later is a half-metal while the former is a near half-metal with spin polarisation of 95%. In the pair Co_2MnSi - Co_2TcSi , the former is a half-metal and the later an ordinary metal. In Figs. 15-17 of supplementary material we show the electronic structures of another three pairs Co_2CrAl - Co_2MoAl , Co_2ScSi - Co_2YSi and Co_2TiSi - Co_2ZrSi respectively. We find that the electronic structures of Co_2TiAl and Co_2ZrAl are identical with the Co states on either sides of the gaps being located even at same energies. Same happens in case of Co_2ScSi - Co_2YSi pair. The differences in the electronic structures near the Fermi levels of Co_2VAl and Co_2NbAl are minimal. Unlike Co_2NbAl , there is a trace of hybridisation between Co and V states around the Fermi level reducing the spin polarisation by a few percent than that of an ideal half-metal. A major difference is observed between Co_2MnSi and Co_2TcSi . This, clearly, is due to the different crystal structures (Co_2MnSi has structure type T_{I} , Co_2TcSi has

structure type T_{II}), the reflections are there in the densities of states. Similar is the case with Co_2CrSi ⁶³ and Co_2MoSi . Analysing the cases where both members of an isoelectronic pair crystallise in structure type T_I but one of them is a half-metal while the other is a metal with medium spin polarisation (Figs 15, 17 of supplementary material), we find that the electronic structures are very similar for the compounds in a pair. For example, in both $Co_2TiSi-Co_2ZrSi$ and $Co_2CrAl-Co_2MoAl$ pairs, the noteworthy feature in the densities of states is the presence of a clear gap in the spin down bands. The differences in the spin polarisation arise due to different positions of the Fermi levels. In Co_2TiSi , the bottom of the conduction band which consists of e_g states of Co falls behind the Fermi level while they are above the Fermi level in Co_2ZrSi . Similar is the case with the other pair of compounds.

IV. CONCLUSIONS

Employing first-principles electronic structure calculations we have systematically studied the structural, electronic and magnetic properties of 54 $X_2X'Z$ ternary Heusler compounds where $X = Mn, Fe, Co$; $Z = Al, Si$ and X' represents 9 elements with $4d$ electrons in their valance shells. In pursuit of finding new half-metallic magnets from ternary series with both $3d$ and $4d$ electrons in the same compounds we found only seven half-metals Mn_2NbAl , Mn_2ZrSi , Mn_2RhSi , Co_2ZrAl , Co_2NbAl , Co_2YSi and Co_2ZrSi with 100% spin polarisation. We also find the compounds Mn_2TcAl , Mn_2RuAl , Mn_2NbSi , Mn_2RuSi , Fe_2NbSi with high spin polarisation (greater than 90%) and a gap like feature in one of the spin-channel near the Fermi-level. These compounds can be identified as “near half-metals”. Tuning the positions of their Fermi levels by application of pressure such that the gap cuts through the Fermi levels may induce half-metallicity in them.

From the present study the hybridisation picture that has been in use to explain the origin of half-metallicity in ternary Heusler compounds with magnetic components being the ones with $3d$ elements only, is found to be valid in case of compounds with both $3d$ and $4d$ elements as constituents. This leads to a general framework in understanding the origin of half-metallic behaviour in Heusler

$X_2X'Z$ compounds where X' can be either a $3d$ element or one from the group of $4d$. An one-on-one comparison between $X_2X'Z$ compounds where X' is a $3d$ element in one case and a $4d$ element in other, shows that as long as N_V , the number of valence electrons are same, the electronic properties like half-metallicity or near half-metallicity with high spin polarisation, by an large, remain intact if a $4d$ element replaces a $3d$ one as X' provided both compounds crystallise in the same ground state structure. Even in cases where the spin polarisations, and subsequent half-metallic features are different, the electronic structures are very similar for compounds with same N_V and same structure type. The differences in electronic properties in regard to half-metallicity occurs due to the relative positions of the bottom of the conduction band and the Fermi energy which is a consequence of the positions of the X and X' states near the Fermi level. Therefore, N_V can be a good predictor to explore possible new half-metals.

The trends in the Curie temperature, T_c , in the compounds with X' a $4d$ element, is found to be correlated with the trends in the dominant exchange interactions. We find that across the series, the $X-X$ exchange interactions determine the trends in T_c for compounds with structure type T_I which in turn can be correlated to the dominance of $X-X$ hybridisations in their electronic structures. In case of compounds with structure type T_{II} , the dominant exchange interactions are X_I-X_{II} and $X_{II}-X'$ deciding the trends in T_c . This, once again, can be correlated to the dominant hybridisations in their electronic structures. The present work, thus, systematically explores the physics behind occurrence of half-metallicity in compounds with magnetic constituents from both $3d$ and $4d$ series and provides with a generalised microscopic picture applicable to a large number of heusler compounds. This would be useful for experimentalists in particular, to explore new materials with novel magnetic applications.

ACKNOWLEDGMENT

We thank Dr. Ashis Kundu for useful discussion and fruitful inputs through out this work. IIT Guwahati and DST India is acknowledged for providing the PARAM superconducting facility and the computer cluster in the Department of Physics, IIT Guwhati.

* Electronic address: subhra@iitg.ac.in

¹ M. Katsnelson, Rev. Mod. Phys. **80**, 315 (2008).

² I. Galanakis, P. H. Dederichs, and N. Papanikolaou, Phys. Rev. B **66**, 134428 (2002).

³ J. Pons, E. Cesari, C. Segu, F. Masdeu, and R. Santamarta, Mat. Sci. Engg. A **481482**, 57 (2008).

⁴ I. Galanakis, P. H. Dederichs, and N. Papanikolaou, Phys. Rev. B **66**, 174429 (2002).

⁵ A. Planes, L. Maosa, and M. Acet, J. Phys.: Condens. Matter **21**, 233201 (2009).

⁶ D. Do, M.-S. Lee, and S. D. Mahanti, Phys. Rev. B **84**, 125104 (2011).

⁷ M. Ramsteiner, O. Brandt, T. Flissikowski, H. Grahm, M. Hashimoto, J. Herfort, and H. Kostial, Physical Review B **78**, 121303 (2008).

⁸ X. Wang, Physical review letters **100**, 156404 (2008).

⁹ X.-L. Wang, S. X. Dou, and C. Zhang, NPG Asia Materials **2**, 31 (2010).

¹⁰ J. Winterlik, G. H. Fecher, A. Thomas, and C. Felser, Physical Review B **79**, 064508 (2009).

- ¹¹ S. Ouardi et al., *Applied Physics Letters* **98**, 211901 (2011).
- ¹² H. Kurt, K. Rode, M. Venkatesan, P. Stamenov, and J. M. D. Coey, *Physical Review B* **83**, 020405 (2011).
- ¹³ V. Alijani, O. Meshcheriakova, J. Winterlik, G. Kreiner, G. H. Fecher, and C. Felser, *J. Appl. Phys.* **113**, 063904 (2013).
- ¹⁴ O. Meshcheriakova et al., *Phys. Rev. Lett.* **113**, 087203 (2014).
- ¹⁵ V. Alijani, J. Winterlik, G. H. Fecher, S. S. Naghavi, S. Chadov, T. Gruhn, and C. Felser, *J. Phys.: Condens. Matter* **24**, 046001.
- ¹⁶ I. Galanakis, K. Özdoğan, E. Şaşıoğlu, and S. Blügel, *J. Appl. Phys.* **116**, 033903 (2014).
- ¹⁷ K. Endo, T. Kanomata, H. Nishihara, and K. Ziebeck, *J. Alloys Compd.* **510**, 1 (2012).
- ¹⁸ T. Graf, C. Felser, and S. S. Parkin, *Prog. Solid State Chem.* **39**, 1 (2011).
- ¹⁹ L. Wollmann, S. Chadov, J. Kübler, and C. Felser, *Phys. Rev. B* **90**, 214420 (2014).
- ²⁰ S. Wurmehl, G. H. Fecher, H. C. Kandpal, V. Ksenofontov, C. Felser, and H.-J. Lin, *Applied physics letters* **88**, 032503 (2006).
- ²¹ R. Weht and W. E. Pickett, *Physical Review B* **60**, 13006 (1999).
- ²² E. Şaşıoğlu, L. Sandratskii, and P. Bruno, *Journal of Physics: Condensed Matter* **17**, 995 (2005).
- ²³ T. Gasi et al., *Physical Review B* **87**, 064411 (2013).
- ²⁴ P. E. Blöchl, *Phys. Rev. B* **50**, 17953 (1994).
- ²⁵ G. Kresse and J. Furthmüller, *Phys. Rev. B* **54**, 11169 (1996).
- ²⁶ G. Kresse and D. Joubert, *Phys. Rev. B* **59**, 1758 (1999).
- ²⁷ J. P. Perdew, K. Burke, and M. Ernzerhof, *Phys. Rev. Lett.* **77**, 3865 (1996).
- ²⁸ M. Methfessel and A. T. Paxton, *Phys. Rev. B* **40**, 3616 (1989).
- ²⁹ H. Ebert, D. Koedderitzsch, and J. Minar, *Rep. Prog. Phys.* **74**, 096501 (2011).
- ³⁰ A. Liechtenstein, M. Katsnelson, V. Antropov, and V. Gubanov, *J. Magn. Magn. Mater.* **67**, 65 (1987).
- ³¹ V. V. Sokolovskiy, V. D. Buchelnikov, M. A. Zagrebin, P. Entel, S. Sahoo, and M. Ogura, *Phys. Rev. B* **86**, 134418 (2012).
- ³² V. Alijani, J. Winterlik, G. H. Fecher, S. S. Naghavi, and C. Felser, *Phys. Rev. B* **83**, 184428 (2011).
- ³³ L. Bainsla et al., *Phys. Rev. B* **92**, 045201 (2015).
- ³⁴ Enamullah, Y. Venkateswara, S. Gupta, M. R. Varma, P. Singh, K. G. Suresh, and A. Alam, *Phys. Rev. B* **92**, 224413 (2015).
- ³⁵ P. Klaer, B. Balke, V. Alijani, J. Winterlik, G. H. Fecher, C. Felser, and H. J. Elmers, *Phys. Rev. B* **84**, 144413 (2011).
- ³⁶ X. Dai, G. Liu, G. H. Fecher, C. Felser, Y. Li, and H. Liu, *J. Appl. Phys.* **105**, 07E901 (2009).
- ³⁷ L. Bainsla et al., *Phys. Rev. B* **91**, 104408 (2015).
- ³⁸ S. Berri, D. Maouche, M. Ibrir, and F. Zerarga, *J. Magn. Magn. Mater.* **354**, 65 (2014).
- ³⁹ Q. Gao, H.-H. Xie, L. Li, G. Lei, J.-B. Deng, and X.-R. Hu, *Superlattices Microstruct.* **85**, 536 (2015).
- ⁴⁰ L. Xiong, L. Yi, and G. Gao, *J. Magn. Magn. Mater.* **360**, 98 (2014).
- ⁴¹ S. Izadi and Z. Nourbakhsh, *J. Supercond. Novel Magn.* **24**, 825 (2011).
- ⁴² M. Singh, H. S. Saini, J. Thakur, A. H. Reshak, and M. K. Kashyap, *J. Alloys Compd.* **580**, 201 (2013).
- ⁴³ L. Bainsla et al., *J. Magn. Magn. Mater.* **394**, 82 (2015).
- ⁴⁴ G. Gökoğlu, *Solid. State. Sciences.* **14**, 1273 (2012).
- ⁴⁵ A. Kundu, S. Ghosh, R. Banerjee, S. Ghosh, and B. Sanyal, *Scientific Reports* **7**, 1803 (2017).
- ⁴⁶ N. Kervan, S. Kervan, O. Cankö, M. Atiş, and F. Taşkın, *Journal of Superconductivity and Novel Magnetism* **29**, 187 (2016).
- ⁴⁷ B. Hamad, *Journal of Materials Science* **51**, 10887 (2016).
- ⁴⁸ A. Abada, K. Amara, S. Hiadsi, and B. Amrani, *Journal of Magnetism and Magnetic Materials* **388**, 59 (2015).
- ⁴⁹ P. Patel, S. B. Pillai, S. Shinde, S. Gupta, and P. K. Jha, *Physica B: Condensed Matter* **550**, 376 (2018).
- ⁵⁰ J.-Y. Jong, J. Zhu, M.-G. Jon, Y. Zhou, J. Kim, and J. Yan, *Journal of Alloys and Compounds* **693**, 462 (2017).
- ⁵¹ J. C. Slater, *Phys. Rev.* **49**, 537 (1936).
- ⁵² L. Pauling, *Phys. Rev.* **54**, 899 (1938).
- ⁵³ S. Skafrouros, K. Özdoğan, E. Şaşıoğlu, and I. Galanakis, *Phys. Rev. B* **87**, 024420 (2013).
- ⁵⁴ I. Galanakis, *Theory of Heusler and Full-Heusler Compounds*, pages 3–36, Springer International Publishing, Cham, 2016.
- ⁵⁵ J. Ma et al., *arXiv preprint arXiv:1712.02278* (2017).
- ⁵⁶ K. Özdoğan, E. Şaşıoğlu, and I. Galanakis, *J. Appl. Phys.* **113**, 193903 (2013).
- ⁵⁷ L. Bouckaert, *Phys. Rev.* **50**, 58 (1936).
- ⁵⁸ M. E. Jamer et al., *Physical Review Applied* **7**, 064036 (2017).
- ⁵⁹ H. C. Kandpal, C. Felser, and G. H. Fecher, *Journal of Magnetism and Magnetic Materials* **310**, 1626 (2007).
- ⁶⁰ M. Zagrebin, V. Sokolovskiy, and V. Buchelnikov, *Journal of Physics D: Applied Physics* **49**, 355004 (2016).
- ⁶¹ J. Kübler, G. H. Fecher, and C. Felser, *Phys. Rev. B* **76**, 024414 (2007).
- ⁶² E. Shreder, A. Svyazhin, and S. Streltsov, *Phys. Met. Metallogr* **100**, S5 (2005).
- ⁶³ D. P. Rai et al., *Bulletin of Materials Science* **34**, 1219 (2011).